

GT2011-4) ' %

HIGH FREQUENCY PRESSURE MEASUREMENTS WITH AN UNCOOLED FAST INSERTION PROBE AT TURBINE EXIT IN A TURBOJET ENGINE

R.J. Lubbock and M.L.G. Oldfield
Osney Thermo-fluids Laboratory,
Department of Engineering Science,
University of Oxford, UK

ABSTRACT

This paper concerns the development and testing of a novel high frequency pressure probe for high temperature turbomachinery flow measurements. The probe has a measurement bandwidth from DC to 100 kHz and has been demonstrated in conditions of up to 6 bar and 1900 K. The 4 mm diameter probes are uncooled whilst in the flow and employ a fast insertion traverse to limit immersion times to of the order of 0.1 seconds. The probe was calibrated against a hot wire anemometer in a known turbulent flow. Data acquired downstream of the turbine in a turbojet engine is presented. The unsteady pressure data is decomposed into periodic and random components. Power spectra, turbulence intensity and length scale are derived. Short duration gas turbine measurements using fast insertion techniques have been under development for some years at the University of Oxford. The current fast-insertion probe is more compact and robust than previous designs. The present work demonstrates that it can resolve useful flow parameters in hostile gas turbine flows. These can be difficult or impossible to obtain using other methods. The rapid probe insertion technique should add to the armoury of diagnostic tools used by the gas turbine developer.

NOMENCLATURE

f	frequency
$F(f)$	frequency calibration function
$G(k)$	wavenumber calibration function
$H(\bar{U})$	velocity calibration function
k	wavenumber
L_x	turbulence integral length scale
$M(k, \bar{U})$	turbulence spectrum measured by probe
\bar{P}_0	time-average total pressure
P_{ac}	unsteady total pressure
\tilde{P}_0	periodic component of unsteady total pressure
P'_0	quasi-random component of unsteady total pressure

\bar{p}	time-average static pressure
$S(k)$	turbulence spectrum measured by hot wire
T	temperature
Tu	turbulence intensity
u'	fluctuating component of stream-wise velocity
\bar{U}	time-average stream-wise velocity
y	Kulite radial position with respect to hub

Abbreviations

BPF	Blade Passing Frequency
FFT	Fast Fourier Transform
FSO	Full Scale Output
HPF	High Pass Filtered
HW	Hot Wire
NGV	Nozzle Guide Vane
P2	Probe 2
PLA	Phase Locked Average
PSD	Power Spectral Density
RMS	Root Mean Square

INTRODUCTION

It is widely accepted that combustor generated turbulence significantly enhances heat transfer to gas turbine Nozzle Guide Vanes and turbine blades (see e.g. [1] and [2] for recent reviews). It has been shown that the Nusselt number is a function of both turbulence intensity and integral length scale [3], with enhancement factors of up to 40% possible [4, 5]. Component lifetime may be reduced by several percent for just a single degree increase in component metal temperature [6, 7]. Knowledge of the unsteady flow field from which these turbulence parameters are derived is therefore critical in order to improve cycle performance and increase component life.

The gas turbine flow field is extremely complex and highly unsteady, and at present cannot be adequately resolved by CFD methods. Measurements are necessary to evaluate component

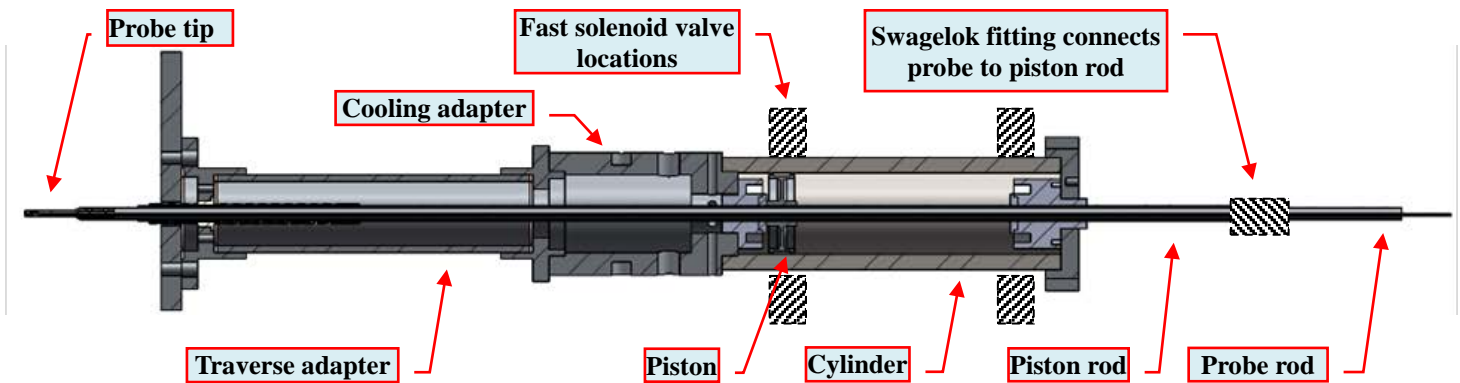


Figure 1: schematic cross-section of fast-insertion probe-traverse system.

designs and improve numerical predictions. The hostile operating conditions and high bandwidth requirement make such measurements very challenging, particularly in the hot section where the requirement is greatest. Poor optical access and the presence of combustion products together make optical techniques impractical, therefore intrusive techniques are required. Traditionally, unsteady flow velocity is measured using hot wires, however these are far too fragile for use in an engine. The alternative is to use aerodynamic probes which are robust and relatively low cost. Comprehensive reviews of unsteady turbomachinery probe measurement techniques are given by both Ainsworth et al. [8] and Sieverding et al. [9]. However, the majority of these techniques are designed for use in cascades and short duration test facilities.

There are very few probes capable of making high frequency (DC to 100 kHz) measurements in engine environments. In order to maximise frequency response the pressure sensing element must be flush mounted on the probe tip. However, this also exposes it to the hot gas. Whilst piezoresistive sensors capable of withstanding temperatures up to 870 K have been reported [10] these are not yet available in a sufficiently compact commercial package to enable installation in a miniature probe. Furthermore, they would not survive in the majority of engine flows without some sort of thermal protection.

Two methods have been developed that allow commercially available, lower temperature (550 K), piezoresistive sensors to be used. The approach adopted by Brouckaert, Mersinligil et al. [11, 12] is to water cool the sensor and probe body. This probe has the advantage of being able to withstand continuous immersion, thus enabling it to make complete radial traverses with varying yaw angle. However its application to the hottest flows is limited by the rate with which heat can be removed from the sensor. These probes have proven feasible in moderately high Nusselt number flows (1900 K, 2 bar). However, in spite of substantial cooling apparatus, they still suffer from thermally induced inaccuracy.

The alternative approach pioneered by Moss [7] and subsequently developed by Passaro et al. [13, 14] is to traverse the sensor across the hot gas path rapidly so that it remains within its thermal limits throughout the traverse. The probes

themselves do not require internal cooling, making them simpler to manufacture and cheaper to replace. The advantage of this technique is that the probe immersion time may be adjusted to suit even the most severe turbomachinery flows.

This paper demonstrates that it is possible to measure the unsteady pressure fluctuations, and hence turbulence, downstream of the turbine in a hostile engine environment using uncooled fast insertion probes.

PROBE DESCRIPTION

High-temperature fast-insertion probes have been the subject of development at Oxford during the past two decades [15]. The pneumatically driven fast-insertion technique employs a rapidly-actuated traverse mechanism (Figure 1) to insert the probe into the flow for short periods and retract it before the probe undergoes any irreversible thermal effects. The design of the original fast-insertion traverse is described by Battelle [16], whilst extensive re-design and improvements are described by Passaro et al. [14]. The design and operation of the current traverse is described in detail by these authors, and will briefly be summarized here.

The traverse employs a pneumatically actuated piston controlled by four fast solenoid valves to insert and retract the probes radially in relation to the engine. These valves are triggered by two digital pulses from the data acquisition system (one to open and close the ‘push’ valve pair, and one to open and close the ‘pull’ valve pair). The maximum stroke is approximately 120 mm and a typical insertion lasts about 0.3 s, during which the probe is stationary at full insertion for approximately 0.1 s. Once retracted the probe is shielded from the hot flow by a stream of ambient temperature air. The probe itself is uncooled whilst in the flow. The shielding air is fed into the traverse through the cooling adapter, and mass flow is controlled using a choked orifice fitting in the air feed line. The probe position is measured using a linear potentiometer mounted on the traverse. The probe trajectory can be controlled, albeit rather crudely, by adjusting the regulated driving pressure, typically between 3 and 6 bar. The maximum probe stem diameter is 10 mm and the probes are secured and sealed to the traverse using a modified Swagelok fitting. This



Figure 2: The Fast-Insertion Pressure Probe. Sensors from right to left are the Kulite XCE-77-062-10BARA high frequency transducer, the 125 μm K-type thermocouple and the Pitot tube.

allows the probes to be quickly swapped without removing the traverse.

The present probe was designed to be more compact and more robust than previous designs, whilst maintaining compatibility with the existing fast-insertion traverse mechanism. The Kulite Ultra-miniature XCE-77-062-10BARA piezoresistive pressure transducer [17] was selected for its high bandwidth (DC to 100 kHz), small size (1.6 mm diameter), high temperature capability and proven robustness in combustor flows [7], [13]. This sensor is capable of continuous operation at temperatures up to 546 K because the piezoresistive sensing elements are dielectrically isolated from the silicon diaphragm to which they are attached (see for example [18]). A Kulite ‘B’ screen and paralene diaphragm coating were specified in order to protect the diaphragm from particle impacts in the dirty engine flow. On exposure to the hot gas flow the transient temperature distribution within the Kulite diaphragm induces stresses in opposition to those induced by the pressure force acting on the diaphragm. This transient thermal ‘drift’ is well known [7]. However, it cannot be corrected and so the Kulite is only able to measure the unsteady total pressure component. A Pitot tube is therefore installed in close vicinity to the Kulite in order to transmit the low frequency average total pressure to a low frequency transducer mounted on the traverse system approximately one meter from the probe tip. A K-type thermocouple is also mounted on the probe tip in order to monitor the gas temperature in the vicinity of the Kulite whilst the probe is retracted, and to give some indication of the gas path temperature. The Kulite, Pitot tube and a 125 μm (0.005”) diameter thermocouple were mounted slightly proud of the 4 mm diameter stainless steel tip and held in place using high temperature ceramic adhesive. The tip and probe body were designed to minimise both aerodynamic loads due to the high speed flow (the present probe was designed to withstand a Mach number of 0.6 at a total pressure of 8 bar) and inertial loads due to the fast-insertion, during which probe deceleration is approximately 5g. A second 125 μm K-type thermocouple was also installed immediately behind the Kulite transducer in order to monitor the temperature around the fragile Kulite leads. The completed probe is shown in Figure 2.

Signals from the probe are amplified using low noise preamplifiers developed at the University of Oxford which

have been described in a previous publication [13]. The preamplifiers are situated in the test cell adjacent to the probe, and the signals are then transmitted along BNC cables of up to 25 m in length to the user-operated data acquisition and control PC located remotely for safety reasons. Signals are acquired at the DAQ PC using a National Instruments PCI-6254 data acquisition card, two NI BNC-2020 connector boxes and software written in National Instruments Labview [16], which is also used to control the fast solenoid valves to actuate the traverse. The preamplifiers have three outputs: a DCx10 output, and ACx100 output and an ACx1000 output. The cut-off frequency of the anti-aliasing filter on the AC channels was set to 190 kHz. The amplifiers also have a current sensing circuit which outputs a voltage directly proportional to the Kulite supply current, which is temperature dependent and can therefore be used to monitor the average diaphragm temperature [7].

Turbulence parameters

The total pressure measured by the probe can be converted to stream-wise velocity using the method of Moss and Oldfield [19], who reduced the unsteady form of the Bernoulli equation to the following linear relationship between velocity and total pressure:

$$\frac{u'}{\bar{U}} = \frac{1}{2} \frac{P'_0}{\bar{P}_0 - \bar{p}} \quad (1)$$

They showed that for low turbulence levels the second order unsteady velocity terms can be ignored. Furthermore they assumed that unsteady density fluctuations are small compared to the velocity fluctuations on the basis that the Mach number is also low [3] and that turbulent temperature fluctuations may be ignored, as demonstrated by Moss [20]. Eq. (1) requires knowledge of the time-average static pressure. The current traverse allows the probe to be yawed in 5 degree increments so that it could be operated in virtual three-hole mode [see e.g. 9] to obtain the static pressure. However this is currently a manual adjustment and is therefore impractical in a real engine test situation, when time on the test-bed is often very limited. Instead the static pressure may be obtained either from rig data (if available from a previous measurement survey) or to an approximation from a wall static pressure tapping.

The unsteady pressure downstream of the turbine may be decomposed into a periodic component, due to the blade passing, and a quasi-random component due to the free-stream turbulence. In order to isolate the periodic fluctuations the phase-locked average (PLA) of the unsteady signal is computed by re-sampling the signal at an integer multiple of the blade passing frequency, then cutting the re-sampled signal into a number of segments of equal length (number of samples) corresponding to an integer number of blade passages, and subsequently averaging these segments. Usually a once-per-rev signal is used to determine the start (trigger point) of each revolution. However if the engine speed is known to be

constant during the short probe insertion time the blade passing frequency and hence averaging period may be found using an alternative method as follows: an initial estimate of the BPF is obtained from the FFT of the raw unsteady pressure signal, and the PLA for one blade passing is computed based on this initial BPF estimate. By varying the BPF by one or two multiples of the FFT resolution and re-computing the PLA it is possible to determine the BPF that gives the maximum PLA RMS amplitude.

Once the periodic component has been isolated it is subtracted from the original signal leaving the turbulent pressure component, which is then converted to velocity using Eq. (1). The turbulence parameters are then found using standard methods [3, 7]: The turbulence intensity is found by integrating the wavenumber power spectrum, and the integral length scale is found from integrating the central peak of the autocorrelation function, which is itself found from the inverse FFT of the frequency power spectrum.

CALIBRATION

The probe was calibrated for frequency and wavenumber response against a hot wire anemometer following the method of Moss and Oldfield [19]. The calibration is necessary for two reasons: Firstly, to correct for the resonance of the air in the cavity between the Kulite transducer diaphragm and protective steel B-screen at around 50 kHz, and secondly to correct for the wavenumber response of the Kulite sensor due its finite size (1.6 mm diameter) in comparison with the size of the turbulent flow structures. Tests were performed in an open-circuit wind tunnel with a 150 mm square working section. A horizontal grid consisting of ten parallel 6 mm diameter bars spaced at 15 mm pitch was installed 144 mm upstream in order to generate nearly-isotropic free-stream turbulence at the measurement plane. This configuration was chosen by Moss (using a correlation by Roach [21]) who demonstrated that it produced a spectrum representative of combustor turbulence [20].

The power spectra were measured by a hot wire anemometer at tunnel velocities between 64 m/s and 87 m/s and found to be very similar when plotted in wavenumber space. This means that not only is the turbulence virtually independent of Reynolds number, but, also, that the turbulence spectrum may be considered to be a function of wavenumber only, $S(k)$. Hot wire spectra from three acquisitions at 64 m/s, 74 m/s and 87 m/s were averaged and smoothed slightly to produce the reference spectrum, $S(k)$, for calibration. Sharp peaks due to wire support resonances and electrical interference were removed and replaced by a locally smoothed curve. The spectra measured by the probe were averaged over three acquisitions at both 64 m/s and 87 m/s and also slightly smoothed. Spikes due to an acoustic resonance of the grid bars were found to be

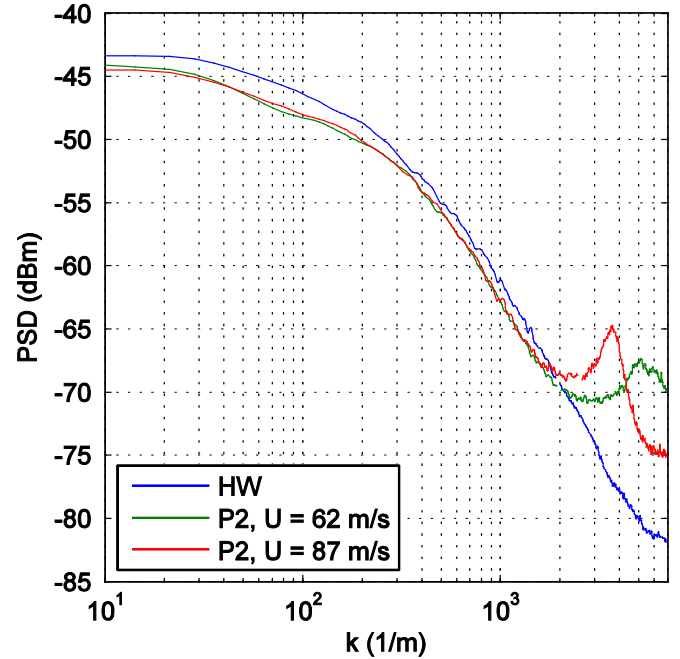


Figure 3: Probe 2 pre-calibration power spectral densities at 62 m/s and 87 m/s compared with the hot wire reference spectra (HW)

present in the probe spectra, and again these were replaced by locally smoothed curves. It was felt that eliminating these experimentally would make little difference to the fidelity of the measured turbulence spectra used for calibration. All data was sampled at 200 kHz for 2 seconds and the Welch power spectrum algorithm was used to compute the power spectra by averaging 64 FFTs of 2048-point Hamming-windowed segments with zero overlap. The hot wire reference spectra and the measured probe spectra at 64 m/s and 87 m/s are shown in Figure 3. The plots indicate that the spectra measured by the probe are a function of wavenumber and mean velocity only, i.e. $M(k, \bar{U})$. It is therefore reasonable to suppose that the measured spectra may be related to the hot wire spectrum, $S(k)$, considered correct, by the following equation [19]:

$$M(k, \bar{U}) = S(k)F(f)G(k)H(\bar{U}) \text{ where } f = \frac{k\bar{U}}{2\pi} \quad (2)$$

At wavenumbers up to approximately 1300 m^{-1} the probe spectra at the two different velocities are virtually identical, therefore it is reasonable to assume that Reynolds and Mach number effects are negligible so that $H(\bar{U}) \approx 1$, and therefore

$$M(k, \bar{U}) = S(k)F(f)G(k) \quad (3)$$

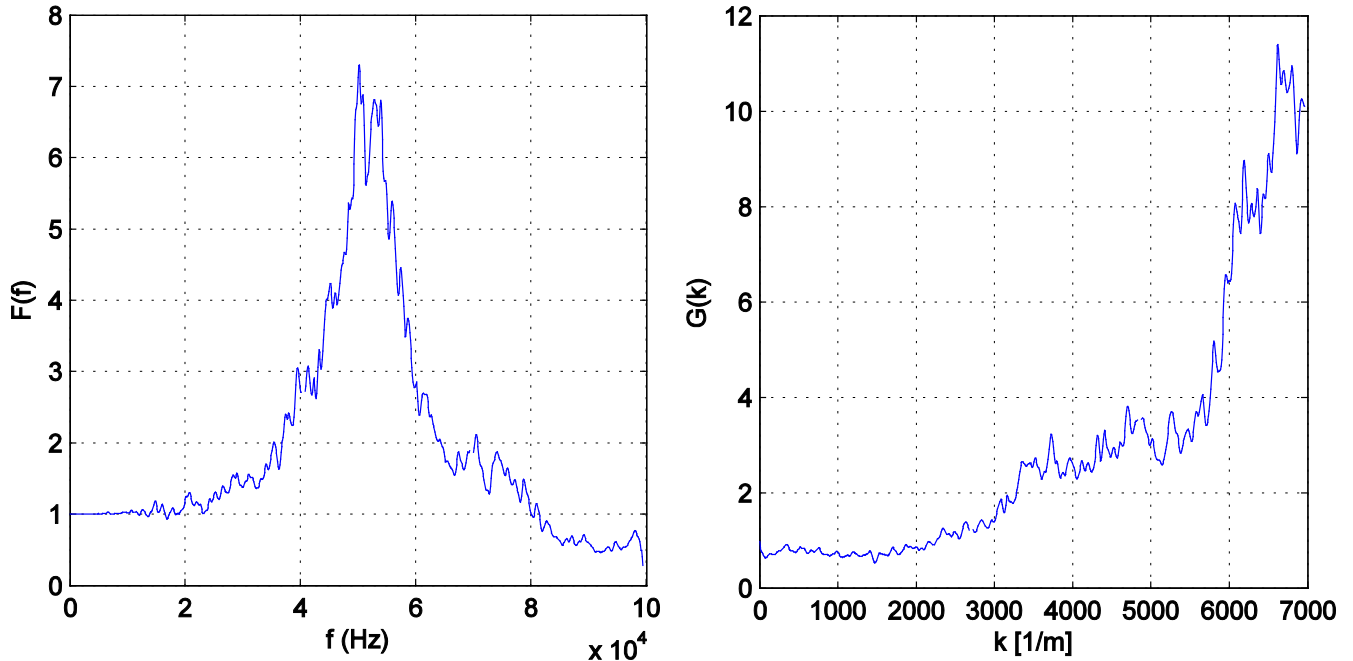


Figure 4: Calibration functions $F(f)$ and $G(k)$ for the spectra in Figure 3.

The method used to obtain the calibration functions is explained at length in [4] and [19]. The calibration functions are plotted in Figure 4. Note that these calibration functions differ from those found in [20] as the probe geometry and diaphragm coating were different.

To demonstrate the validity of the calibration the functions $F(f)$ and $G(k)$ were then applied to the original pressure probe

spectra (after smoothing), and compared with the average hot wire spectrum. The results in Figure 5 show that the calibration procedure is accurate. The average turbulence intensity found from integrating the three hot wire spectra was $9.2\% \pm 0.4\%$. The turbulence intensity from the uncalibrated probe spectra was found to be $8.3\% \pm 0.2\%$, whereas following calibration it was found to be $9.3\% \pm 0.1\%$. The turbulence length scale, found from the inverse FFT of the frequency power spectra,

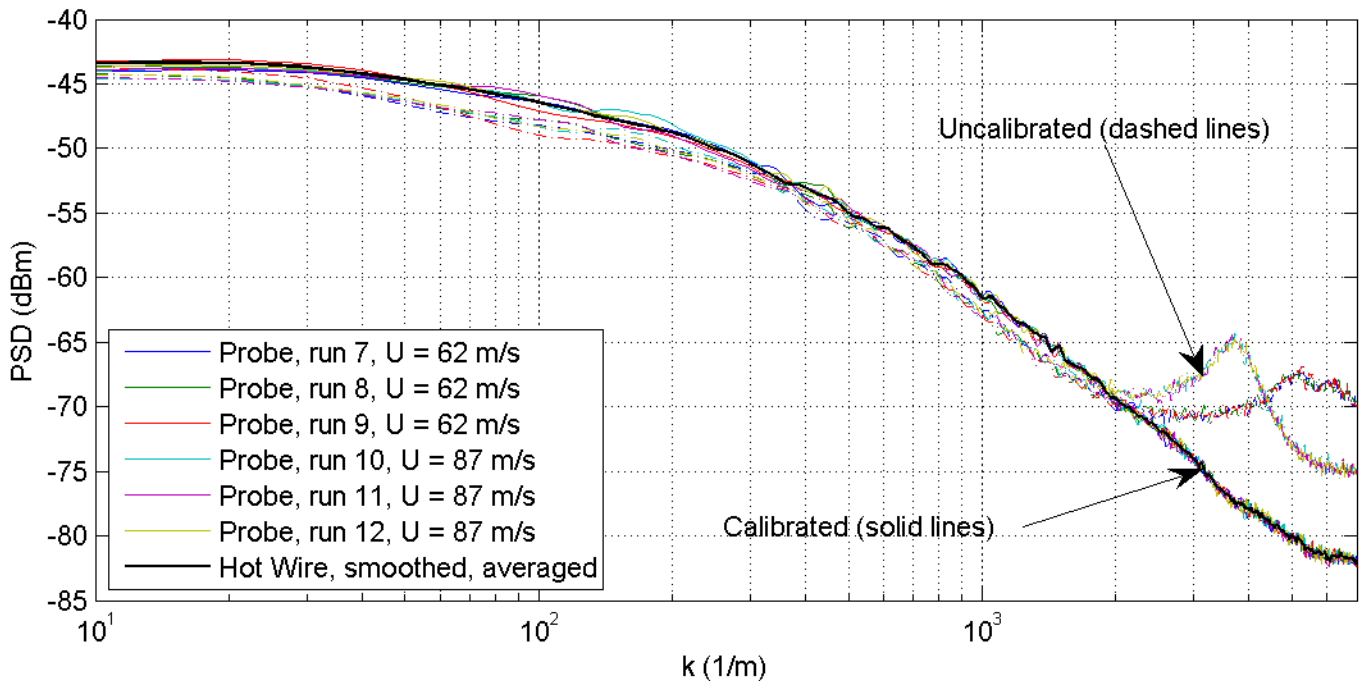


Figure 5: Probe 2 calibrated wavenumber spectra from several runs

was $13.6 \text{ mm} \pm 0.8 \text{ mm}$ for the three hot wire runs. The average length scale from the uncalibrated probe spectra was $15.6 \pm 2.7 \text{ mm}$, whereas for the corrected spectra it was $12.1 \pm 2.1 \text{ mm}$. For measurements of the turbulence parameters of interest, namely intensity and length scale, the calibrated probe is therefore in good agreement with the hot wire, taking into account the data spread. In characterising a highly random process with single numerical values such spreads of data are inevitable.

TEST FACILITY

Tests were conducted at the Scitek Consultants Ltd. engine test facility located at Rolls-Royce, Ansty, UK (Figure 6). The test engine was a Rolls-Royce Viper Mk201C turbojet which produces approximately 10 kN continuous dry thrust at 13000 RPM. The compressor is driven by a single-stage turbine with 113 blades, each measuring 75 mm in height by 17 mm axial chord. The turbine diameter is approximately 500 mm at the blade tip, giving a blade pitch of about 12mm. The traverse was installed on a port on the jet pipe downstream of the turbine (Figure 7) so that the probe axis was 34 mm from the turbine exit plane (Figure 8). A static pressure tapping was also installed in this same axial plane but at a different circumferential position.

Data acquisitions were made at two different frequencies: 100 kHz and 200 kHz. In a 100 kHz acquisition all available signals were acquired, whilst in a 200 kHz acquisition only the less repeatable and high frequency signals were acquired, which allowed the sampling rate per channel to be increased whilst remaining within the limits of the DAQ card. Each 200 kHz acquisition was immediately preceded and/or proceeded by a 100 kHz acquisition, and the repeatable DC values from the 100 kHz acquisition used in processing the 200 kHz signals.

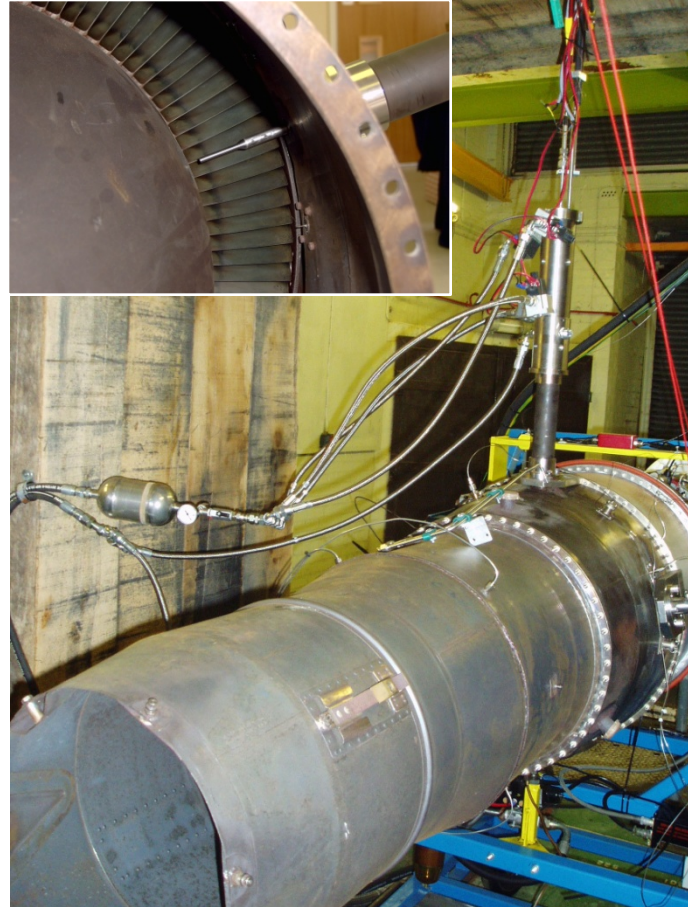


Figure 7: The fast insertion traverse installed on the Viper, and inset on a trial fit, showing the probe relative to the turbine.



Figure 6: The Rolls-Royce Viper Mk201C turbojet with the traverse installed in the vertical position.

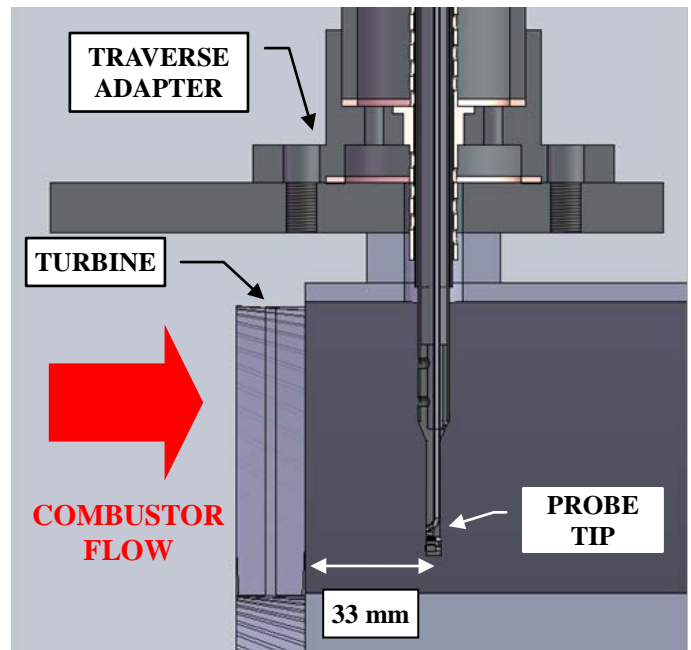


Figure 8: schematic cross-section showing fully inserted probe position relative to turbine.

The insertion system was set to give two different trajectories (Figure 9). In both cases the probe is initially at rest in the retracted position within the air-cooling shroud. In a typical ‘fast’ insertion the probe is inserted to maximum distance where it remains stationary for a set time before being retracted. The ‘slow’ trajectory was obtained by adjusting the driving pressure in order to slowly traverse the probe across the flow in order to obtain profile measurements. Whilst a greater penetration depth would have been desirable, it is difficult to account for the increased frictional forces induced in the insertion system by the aerodynamic loading of the probe, given that the driving pressure must be adjusted manually in the test cell whilst the engine is off. The test schedule did not allow for further adjustment. Future probe and traverse modifications will address this problem.

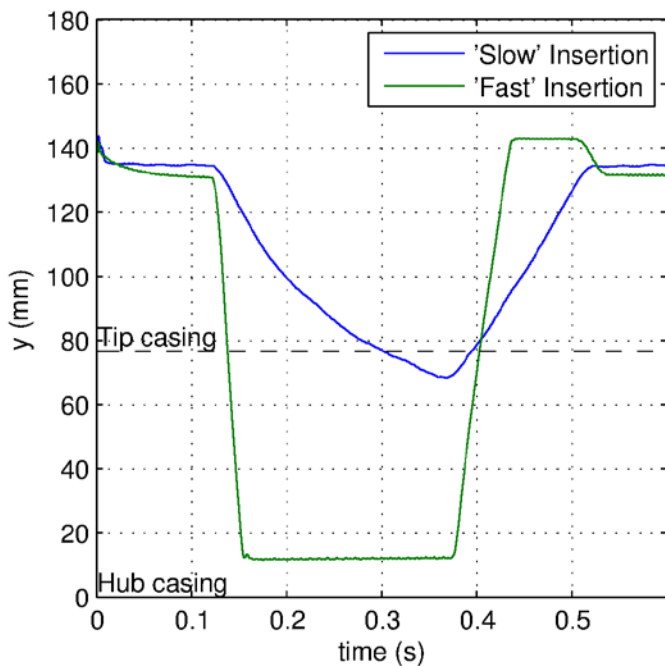


Figure 9: Typical probe trajectories during the tests.

RESULTS

The signals acquired during a typical fast insertion at the maximum engine speed of 12800 RPM are shown in Figure 10. The plot shows the three measured pressure signals: the Pitot steady and Kulite unsteady total pressures, measured by the probe, and the static pressure from the wall pressure tapping. The signals shown are from two subsequent 100 kHz runs (either side of a 200 kHz run) and are plotted together to demonstrate the run-to-run repeatability.

The wall static pressure is slightly above that measured by the probe in the retracted position due to the cooling flow around the probe tip in the retracted position. The Kulite DC pressure exhibits a negative thermal drift as previously discussed. The pitot signal rises sharply and remains flat for the duration of the insertion; therefore, despite being connected to the probe tip by approximately 1 meter of tubing, the transducer

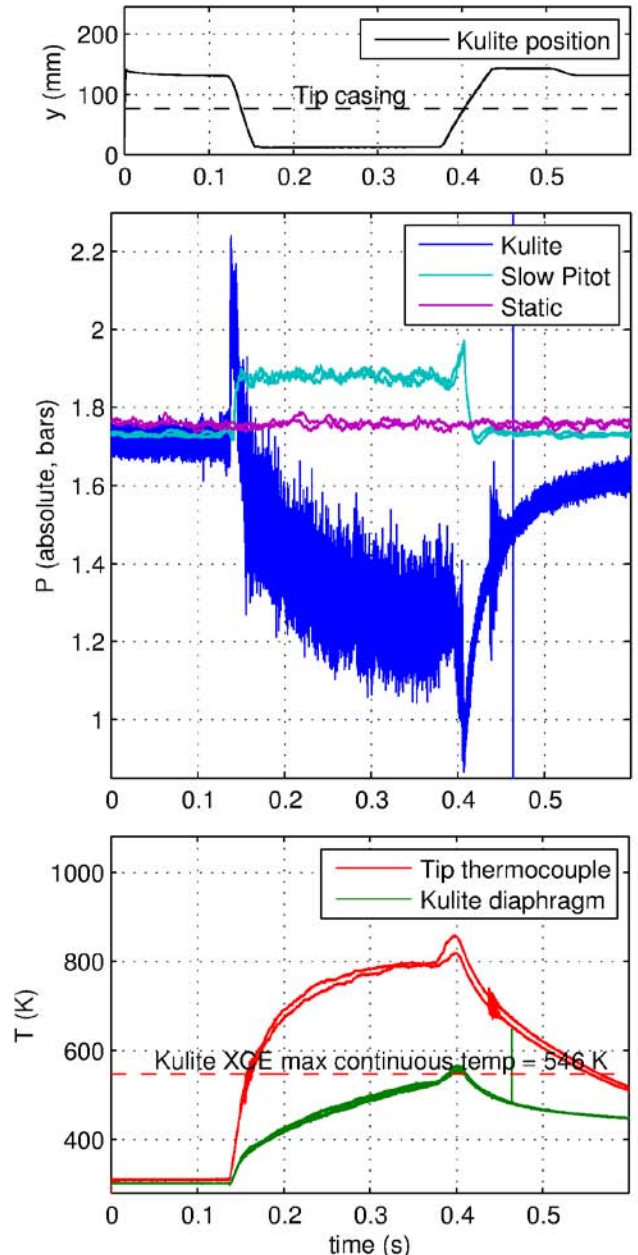


Figure 10: Typical fast insertion signals at 12800 RPM. Traces from two subsequent runs are plotted to demonstrate the run-to-run repeatability.

is responding sufficiently rapidly to the step change in pressure. As well as monitoring the gas temperature when retracted, the gas path thermocouple gives an indication of the gas temperature at the measurement location. The response time of the 125 μm thermocouple bead is not quite fast enough to reach the steady state gas temperature, which does not matter since this measurement does not influence the pressure measurements. Plotted alongside the thermocouple, the approximate average temperature rise of the Kulite diaphragm shows that the diaphragm remains within its continuous operational limit of 546 K for most of the run, and only exceeds

this limit by a small amount (17 K) just before retraction. This does not affect the pressure measurements since the section of data used for the high frequency processing is well before the Kulite reaches its limit. This slight over-temperature for this short time had no lasting effect on the transducer.

In the present test the once-per-rev signal was found to suffer from cross-talk, particularly for the 200 kHz runs. By conditioning the once-per-rev voltage signal from the 100 kHz runs it was possible to determine a peak location for each revolution, and hence find the revolution period and therefore engine speed. This was found to remain constant over the course of each run as expected given the short probe insertion time. The once-per-rev signal from the 200 kHz runs was too badly corrupted to determine the peak locations for most of the signal; therefore the BPF was found using the alternative method as described previously. For the data shown acquired at 12800 RPM the BPF found from the FFT was 24114 Hz and the BPF that maximized the PLA was 24111 Hz. Using a 100 kHz run the alternative technique was compared with simply using the once-per-rev signal to trigger the PLA and it was found that there was virtually no difference in the PLA signal.

The Kulite AC signal was high pass filtered using a second order Butterworth filter (cut-off frequency 200 Hz) in order to remove the thermal drift and any offset. The filtered signal was then cropped to leave only the data points sampled when the probe was at rest at full insertion ($0.17 < t < 0.37$ s). The PLA was computed for one complete revolution by averaging across the total number of revolutions within the cropped re-sampled data. Although the immersion time was short this was still sufficient to capture 42 complete engine revolutions during a

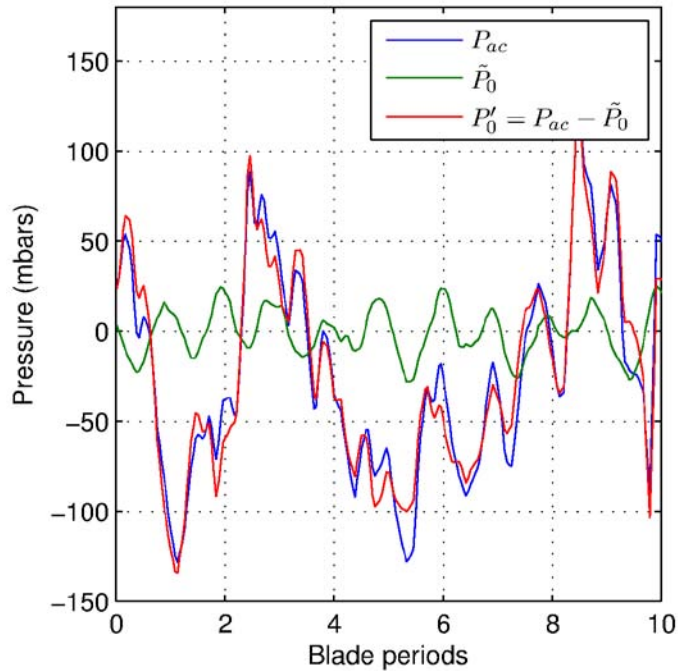


Figure 11: The raw (P_{ac}) and periodic (\tilde{P}_0) total pressure components, and their quasi-random remainder (P'_0) for a fast insertion at 12800 RPM. 10 blade periods shown.

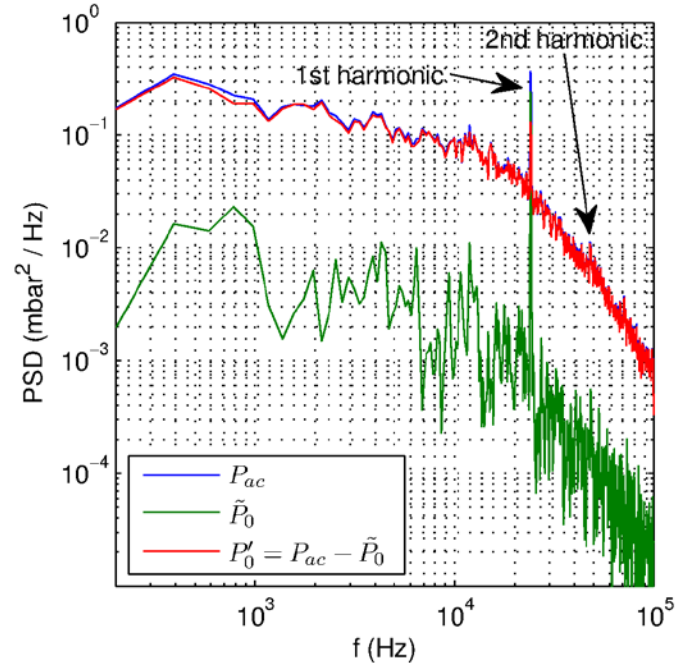


Figure 12: Corrected frequency power spectral density for a fast insertion at 12800 RPM.

fast insertion. The PLA signal was then concatenated to the same length as the original signal and subtracted from it in order to isolate the quasi-random turbulent pressure component. Short samples of 10 blade periods of the original unsteady, periodic and turbulent pressure signals are plotted together in Figure 11. Although most of the peaks in the raw signal coincide with those in the PLA, the RMS amplitude of the PLA is only 13 mbar compared with 51 mbar for the raw signal. This difference in RMS amplitude suggests that in this position at full insertion (approximately 12 mm from the hub) the probe is in the highly turbulent hub boundary layer region. These RMS values are of similar magnitude to the values obtained by Mersinligil et al. [12] on the same engine at the same location, albeit at 10000 RPM.

The power spectral densities of the raw unsteady signal and its two components are computed using the following method: The pressure fluctuations are converted to turbulent fluctuations using Eq. (1) and the raw frequency power (ratio) spectral density is then computed using the Welch power spectrum algorithm by averaging 32 FFTs of 1024-point Hamming-windowed segments with zero overlap. This is then converted to wavenumber and corrected using the frequency and wavenumber calibration functions discussed earlier. The Frequency function found in the calibration was further corrected for the change in sonic velocity in the Kulite air cavity due to the rise in temperature using the correction described by Moss and Oldfield [20], and assuming the cavity air temperature to be the gas path total temperature at the measurement position (from the rig data). The static pressure in this case was obtained from rig data consisting of static pressure measurements made at approximately the same

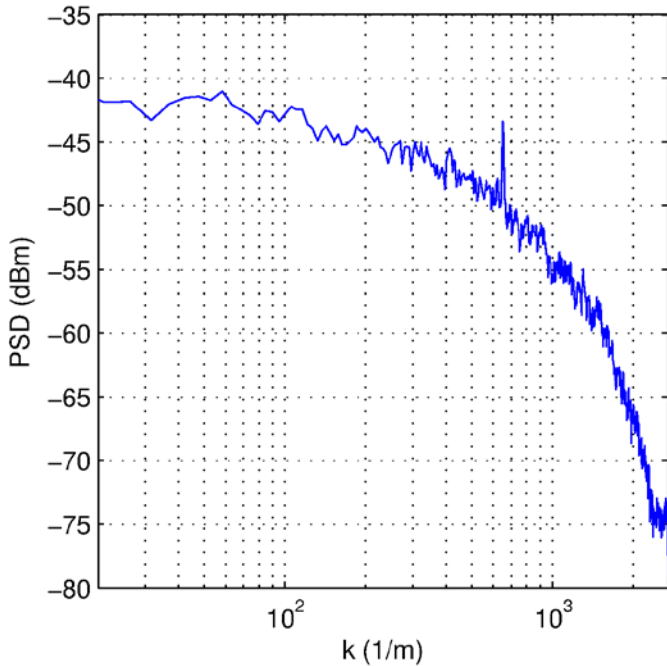


Figure 13: Corrected wavenumber power spectrum for a fast insertion at 12800 RPM.

measurement position. A more accurate measurement might have been obtained from operating the probe in virtual-three-hole mode had sufficient rig testing time been available. Similarly rig data for the temperature at the measurement position was used to compute the mean velocity, although again this could have been obtained using a thermocouple probe immersed for longer times had sufficient rig time been available. The corrected frequency spectrum is then derived from the corrected wavenumber spectrum.

The corrected frequency power spectra are plotted in Figure 12, which shows that subtraction of the PLA signal has almost, but not completely, removed the blade passing fundamental harmonic at around 24 kHz. The second harmonic is also visible in the original signal at around 48 kHz, although it is largely swamped by turbulence. Similarly it is not apparent in the PLA time-domain signal because the small scale periodic flow structures (i.e. low amplitude fluctuations) have largely been swamped by the turbulent fluctuations. Smaller scale periodic flow structure is always going to be attenuated to some extent by averaging because at these scales no two blade passing pressure signatures are identical, due to blade to blade variations and combustor exit flow non-uniformity.

The corrected wavenumber spectrum is shown in Figure 13. The turbulence intensity was obtained from the power spectrum as previously described, and found to be 15.2%. The turbulence length scale was derived from the inverse FFT of the frequency spectrum, itself derived from the corrected wavenumber spectrum. The length scale was found to be 4.5 mm. Turbulence measurements at the exit of a hot combustor exhausting to atmospheric pressure made by Moss [7] revealed intensities of between 8% and 9% and length scales of between

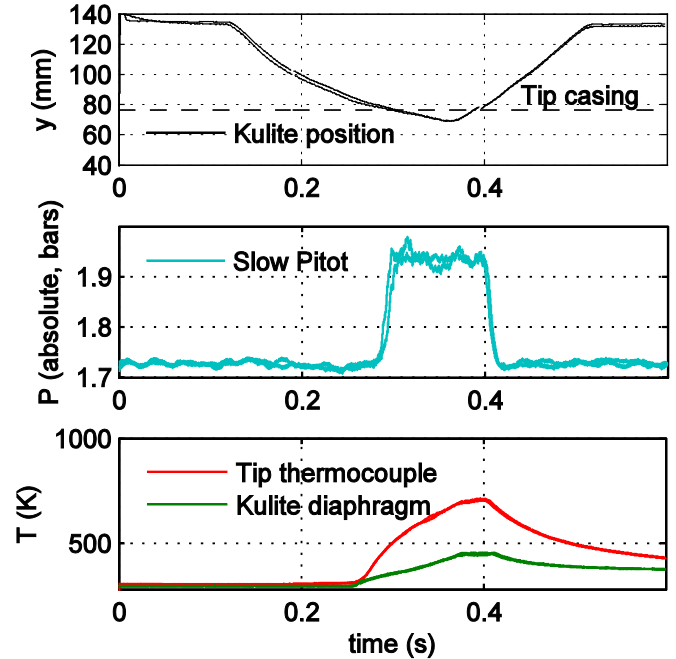


Figure 14: Typical slow insertion signals at 12800 RPM. Traces from two subsequent runs are plotted to demonstrate the run-to-run repeatability.

5.6 mm and 7.6 mm. The present measurements are likely to be different as they are made downstream of the turbine, not at the combustor exit.

The previous analysis was repeated for a slow insertion (Figure 14). Although the probe is clear of the tip casing by at

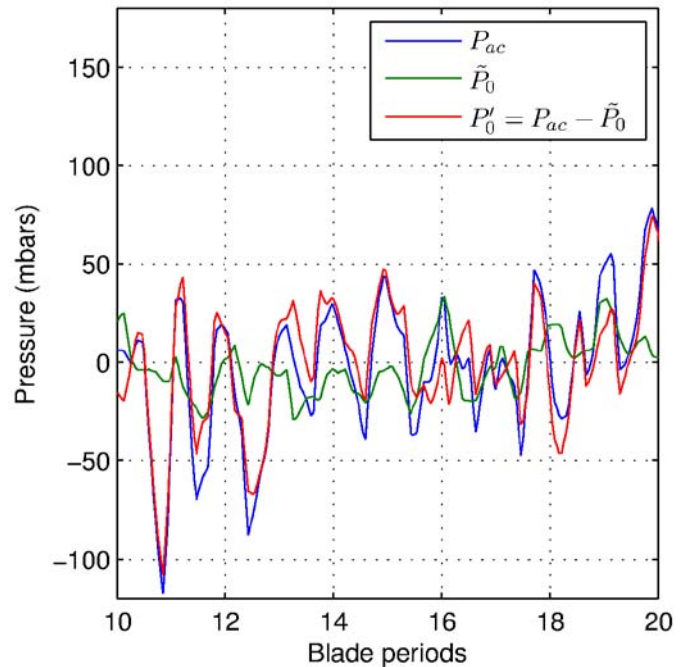


Figure 15: The raw (P_{ac}) and periodic (\tilde{P}_0), total pressure components, and their quasi-random remainder (P'_0) for a slow insertion at 12800 RPM. 10 blade periods shown.

most 10 mm the thermocouple and Pitot pressure signals indicate that in spite of this shallow immersion the probe is clear of the cooling flow and immersed in the hot gas path. This also agrees with the rig data at this position. Figure 15 shows the PLA of this signal compared with the high pass filtered parent signal for 10 blade periods around the point of maximum immersion. The RMS of the PLA in this region is 13 mbar compared with 38 mbar for the raw signal. Compared with the fast insertion value of 51 mbar for the raw signal this again suggests that the probe is immersed in the main gas path as opposed to the boundary layer.

The corrected frequency spectra for the slow insertion are shown in Figure 16. The blade passing second harmonic is much more visible in both the raw and periodic spectra compared with the fast insertion since it is swamped less by the gas path turbulence. The turbulence intensity and length scale were found from the corrected wavenumber power spectrum (plotted alongside the fast insertion spectrum for comparison in Figure 17) to be 12.9% and 6.6 mm respectively. The higher turbulence level for the fast insertion into the more turbulent hub flow is clearly seen.

In total three pressure probes were constructed to the same specifications. These probes each performed around 50 insertions into the Viper turbojet, a Volvo RM12 turbofan (downstream of the LPT) and a Rolls-Royce combustor rig. Conditions in the latter were 1900 K temperature and 6 bar total pressure. During these tests none of the probes suffered any noticeable degradation; they may therefore be considered to be highly rugged.

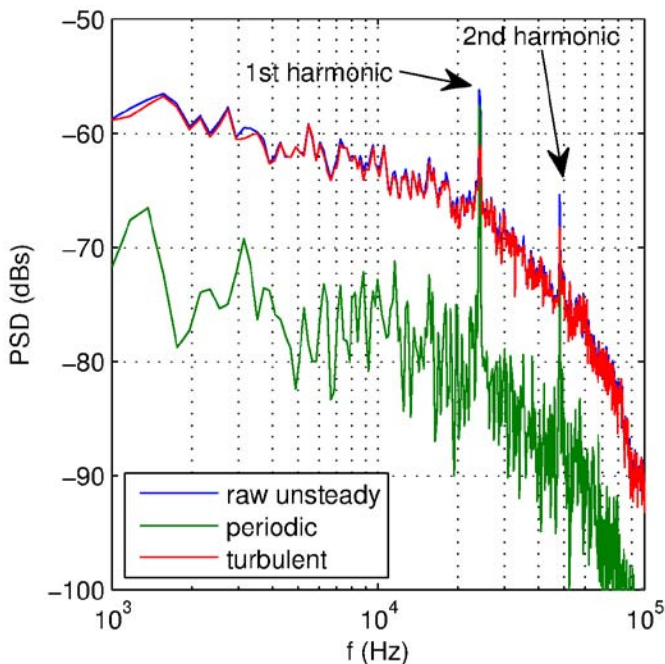


Figure 16: Frequency power spectral densities for a slow insertion at 12800 RPM.

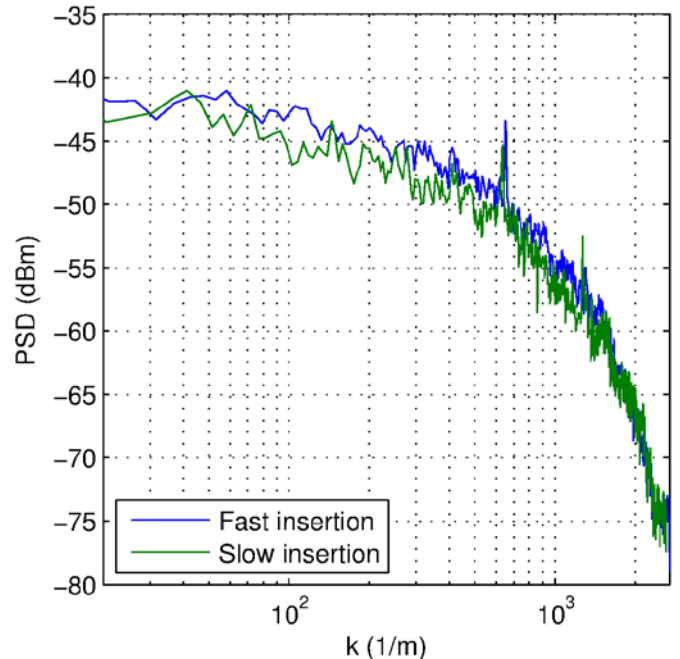


Figure 17: Wavenumber power spectrum for the slow insertion compared with that of the fast insertion from Figure 13.

UNCERTAINTIES AND LIMITATIONS OF THE PRESENT WORK

The maximum error in the unsteady pressure transducer is typically $\pm 0.1\%$ FSO which amounts to 10 mbar for the present Kulite transducer. Similarly the pitot transducer uncertainty is typically $\pm 0.1\%$ FSO which again amounts to 10mbar for the transducer used (the standard deviation on the measured data being 6.5mbar over the time spent at the measurement position). However, the uncertainty in the static pressure measurement is difficult to quantify as wedge probe measurements taken on another test were used. These may not be fully representative of the flow. If more test time had been available, it would have been possible to yaw the probe at different angles and obtain the local static pressure, after calibration, in virtual three-hole mode. Similarly, the probe could have been rotated to determine the flow direction. Based on previously acquired rig data, the flow angle downstream of the Viper turbine was 20° to the axial direction. As the probe was lined up with the axial direction, it is estimated from [21] that the measured mean total pressure would be low by about 3% of the dynamic head. With these considerations, it is estimated that the mean flow velocities measured were probably accurate to only $\pm 6\%$. The PSDs would have a similar accuracy.

The processing used made the assumption that the contribution of temperature and density fluctuations to the velocity turbulence was small compared to that due to the pressure fluctuations, following [19]. A parallel unsteady temperature survey, using thin film gauges, was carried out

during the Viper tests. These have not been fully analysed yet. They should throw light on the assumption made.

It should be emphasised that the main purpose of these tests was to demonstrate that the rapid insertion probe could survive in the harsh, hot, high-pressure gas turbine environment and that meaningful readings could be obtained. The test time in the engine was limited and not all desirable tests could be completed. With this in mind, the tests were a success and the technique shows promise. Now that the concept is proven, future efforts can improve the accuracy of the measurements.

CONCLUSIONS

1. A fast-insertion high frequency pressure probe has been developed that is able to survive in the high temperature, hostile environment downstream of the turbine in a gas turbine operating at nominal conditions.

2. The frequency response of the probe is sufficient to resolve blade passing and finer turbulent flow structures.

3. The measurement time is sufficiently long to compute the phase locked average blade passing signal, which can be removed from the unsteady pressure signal in order to determine the background turbulence level and length scale.

4. Uncooled miniature high frequency fast-insertion pressure probes should be considered for hot-section engine measurements as an alternative to the expensive, cooled, low frequency and bulky probes presently in use.

ACKNOWLEDGMENTS

The research presented herein was supported by the EU 6th Framework Programme project HEATTOP (Accurate High Temperature Engine Aero-Thermal Measurements for Gas Turbine Life Optimization Performance and Condition Monitoring) under Contract No. AST5-CT-2006-030696. The work in this paper was performed under WP4 “Advanced Gas Path Measurements”.

The authors would also like to thank Trevor Godfrey and Dominic Harris of the Osney Thermo-Fluids Lab for their work in building the probes and traverse gear.

REFERENCES

1. Han, J., Dutta, S., and Ekkad, S., 2000, *Gas Turbine Heat Transfer and Cooling Technology*, Taylor & Francis, 1st ed.
2. Nix, A.C., 2003, “Effects of High Intensity, Large Length-Scale Freestream Combustor Exit Turbulence on Heat Transfer in Transonic Turbine Blades”, Ph.D. thesis, Virginia Polytechnic Institute and State University, Blacksburg, VA.
3. Hinze, J.O., 1975, *Turbulence*, McGraw-Hill.
4. Moss, R.W. and Oldfield, M.L.G., 1992, “Measurements of the Effect of free-Stream Turbulence Length Scale on Heat Transfer”, ASME IGTI 1992 Gas Turbine Conference, Cologne, ASME 92-GT-244.
5. Moss, R.W. and Oldfield, M., 1996, “Effect of free-stream turbulence on flat-plate heat flux signals: spectra and eddy transport velocities,” *J. Turbomach*, vol. 118, pp. 461–467.
6. Moon, H. and Glezer, B., 1996, “Application of advanced experimental techniques in the development of a cooled turbine nozzle,” ASME 96-GT-233
7. Moss, R.W., 1992, “The effects of turbulence length scale on heat transfer”, Ph.D. thesis, University of Oxford, (OUEL 1924/92).
8. Ainsworth, R. W., Miller, R. J., Moss, R. W., and Thorpe, S., 2000. “Unsteady Pressure Measurement”. *Meas. Sci. Technol.*, Vol. 11, pp 1055-1076.
9. Sieverding, C., Arts, T., Denos, R., and Brouckaert, J., 2000. “Measurement Techniques for Unsteady Flows in Turbomachines.”. *Experiments in Fluids*, Springer Verlag, Vol.28 (Nr. 5), pp285-321.
10. Ned, A.A., Kurtz, A.D., Beheim, G., Masheeb, F., and Stefanescu, S., 2004, “Improved SiC leadless pressure sensors for high temperature, low and high pressure applications,” in Twenty-first transducer workshop, Lexington, Maryland, June 22–23, 2004.
11. Brouckaert, J., Mersinligil, M., and Pau, M., 2009. “A conceptual design study for a new high temperature fast response cooled total pressure probe”. *Transactions of the ASME, Journal of Engineering for Gas Turbines and Power*, 131(2), March.
12. Mersinligil, M, Brouckaert J-F., Desset, J, 2010, “First unsteady pressure measurements with a fast response cooled total pressure probe in high temperature gas turbine environments.” *Proceedings of the ASME Turbo Expo 2010 Power for Land, Sea and Air June 14-18, 2010, Glasgow, UK. ASME GT2010-23630*
13. Passaro, A., LaGraff, J.E., Oldfield, M.L.G., Biagioni, L., Moss, R.W., and Battelle, R.T., 2003, “Measurement of turbulent pressure and temperature fluctuations in a gas turbine combustor”, (NASA CR-2003-212540).
14. Passaro, A., LaGraff, J.E., Oldfield, M.L.G., and Biagioni, L., 2006, “Fast acting probe for measurement of turbulent pressure and temperature fluctuations in a gas turbine combustor”, in 44th AIAA Aerospace Sciences Meeting

and Exhibit, Reno, Nevada, January, 2006 (AIAA 2006-550).

15. Oldfield, M. L. G. and Lubbock, R. J., 2009, "Fast Insertion Pressure and Temperature Probes", VKI Lecture Series on "Advanced high temperature instrumentation for gas turbine applications", Brussels, May 11-15, 2009.
16. Battelle, R.T., 2001, "Design, optimisation and testing of a rapid traversing pressure transducer for measurement of turbulent spectra in a gas turbine combustion chamber", M.Sc. Thesis, Syracuse University.
17. Kulite High Temperature Ultraminiature IS Pressure Transducer XCE-062 Series Datasheet, Kulite Semiconductor products Inc, New Jersey, USA http://www.kulite.com/pdfs/pdf_Data_Sheets/XCE-062.pdf
18. Kurtz, A.D., Ned, A.A., Goodman, S., Epstein, A.H. "Latest Ruggedized High Temperature Piezoresistive Transducers", NASA 2003 Propulsion Measurement Sensor Development Workshop, Huntsville, Alabama, May 13-15, 2003.
19. Moss, R.W. and Oldfield, M.L.G., 1990, "Comparisons between turbulent spectra measured with fast response pressure transducers and hot wires", Proceedings of the 1990 Symposium on Measuring Techniques for Transonic and Supersonic Flow in Cascades and Turbomachines, Brussels, Sept.1990.
20. Moss, R.W. and Oldfield, M.L.G., 1991, "Measurements of Hot Combustor Spectra", ASME IGTI 1991 Gas Turbine Conference, Orlando, ASME 91-GT-351.
21. Roach, P. 1987, "The generation of nearly isotropic turbulence by means of grids", International Journal of Heat and Fluid Flow, Vol. 8 (2), June.
22. Gracey, W., Letko, W, Russell, W. R., 1951, "Wind tunnel investigation of a number of total pressure tubes at high angles of attack.", NACA TN 2331.